Available online at www.sciencedirect.com
SCIENCE DIRECT®
Carbohydrate Research 339 (2004) 1689–1696
Carbohydrate RESEARCH

Metal-ion interactions with sugars. Crystal structures and FT-IR studies of the $LaCl_3$–ribopyranose and $CeCl_3$–ribopyranose complexes

Yan Lu,[a,*] Guocai Deng,[a,*] Fangming Miao[b] and Zhengming Li[a]

[a]*College of Chemistry, Nankai University, Tianjin 300071, PR China*
[b]*Institute of Crystal Chemistry, Tianjin Normal University, Tianjin 300074, PR China*

Received 26 December 2003; received in revised form 18 March 2004; accepted 16 April 2004

Abstract—Single crystals of $LaCl_3{\cdot}C_5H_{10}O_5{\cdot}5H_2O$ (**1**) and $CeCl_3{\cdot}C_5H_{10}O_5{\cdot}5H_2O$ (**2**) were obtained from ethanol–water solutions and their structures determined by X-ray. The two complexes are isomorphous. Two configurations of complex **1** or complex **2**, as a pair of isomers, were found in each single crystal in a disordered state. The ligand of one of the isomer is α-D-ribopyranose in the $^4C_1$ conformation, the ligand of the other is β-D-ribopyranose in the $^1C_4$ conformation. For complex **1**, the α : β anomeric ratio is 51:49, and for complex **2**, the ratio is 52:48. Both ligands of the two isomers provide three hydroxyl groups in *ax–eq–ax* orientation for coordination. The Ln^{3+} (Ln = La or Ce) ion is nine-coordinated with five Ln–O bonds from water molecules, three Ln–O bonds from hydroxyl groups of the D-ribopyranose, and one Ln–Cl bond from chloride ion. The hydroxyl groups, water molecules, and chloride ions form an extensive hydrogen-bond network. The IR spectral C–C, O–H, C–O, and C–O–H vibrations were observed to be shifted in both the two complexes and the IR results are in accord with those of X-ray diffraction.

Keywords: La–D-ribose complex; Ce–D-ribose complex; Crystal structure; FT-IR

1. Introduction

Saccharides are widely distributed in the biosphere, along with proteins and nucleic acids.[1] The multiple oxygen donor atoms in sugar molecules and the fact that metal cations coexist in biological fluids, suggest that coordination between saccharides may have biological relevance. Thus the formation of a Ni^{2+}–carbohydrate complex in human kidney was demonstrated in 1985.[2] Such interactions may have importance in such biochemical processes as the transfer and storage of metal ions,[3,4] the action of metal-containing pharmaceuticals, toxic-metal metabolism,[5,6] and Ca^{2+}-mediated carbohydrate–protein binding.[7,8]

Information in the literature, on the interactions of saccharides with metal cations is rather limited, especially for well-characterized solid complexes, with most previous work being focused on aqueous solution chemistry. Thus far, only the following neutral sugar–metal complexes have been determined by X-ray diffraction: the complexes of Mo^{6+}–D-xylose,[9] Ca^{2+}–D-fructose,[10–12] Ca^{2+}–D-galactose,[13] Ca^{2+}–lactose,[14,15] Na^+–sucrose,[16,17] Na^+–cellobiose,[18] Ca^{2+}–D-mannose,[19] Ca^{2+}–trehalose,[20] Ca^{2+}–D-xylose,[21] Ca^{2+}–L-arabinose,[22] Pr^{3+}–D-ribose,[23] Nd^{3+}–D-ribose,[24,25] and Ca^{2+}–D-ribose.[26] The detailed three-dimensional structures of the saccharides and the role of metal ions in determining and regulating these structures remains obscure.

D-Ribose ($C_5H_{10}O_5$), is important as a component of nucleic acids, and its metal-ion-binding properties may have biological significance. D-Ribose exists in aqueous solution as an equilibrium mixture of six tautomer. Among these, those having an *ax–eq–ax* sequence of

* Corresponding authors. Tel.: +86-22-23503632; e-mail: luuyann@vip.sina.com

0008-6215/$ - see front matter © 2004 Elsevier Ltd. All rights reserved.
doi:10.1016/j.carres.2004.04.009

three adjacent hydroxyl groups coordinated readily with metal cations to form 1:1 complexes in hydrophilic solvents. It has been reported that the 'complexing' isomers constitute altogether 43% of the total, being less only for those of talose.[27] The interactions of Ca^{2+}, Sr^{2+}, Ba^{2+}, La^{3+}, Ce^{3+}, Pr^{3+}, Nd^{3+}, Sm^{3+}, Eu^{3+}, Gd^{3+}, and Tb^{3+} with D-ribose in neutral solutions have been studied by NMR and calorimetric methods,[28–30] and the stability constants have been calculated (<10 M^{-1} in most cases). However, the structures of most of these complexes are still undefined, because solid complexes are difficult to obtain. Since the crystal structure of $PrCl_3 \cdot C_5H_{10}O_5 \cdot 5H_2O$ was reported in 2001, only four such ribose–metal complexes, from Ca^{2+}, La^{3+},[31] Pr^{3+}, and Nd^{3+}, have so far been obtained as solids. No crystal data for the La^{3+}–ribose complex have been reported.

We have obtain single crystals of the La^{3+} and Ce^{3+} complexes with D-ribose, and crystal structures of $LaCl_3 \cdot C_5H_{10}O_5 \cdot 5H_2O$ (**1**) and $CeCl_3 \cdot C_5H_{10}O_5 \cdot 5H_2O$ (**2**) were determined by X-ray. In contrast to the single configuration observed in the single crystals of $PrCl_3 \cdot C_5H_{10}O_5 \cdot 5H_2O$[23] and $NdCl_3 \cdot C_5H_{10}O_5 \cdot 5H_2O$,[24] as reported by Yang et al., two configurations were observed in the single crystals of both **1** and **2**. The configurations reported in this article are similar to those observed in single crystals of $NdCl_3 \cdot C_5H_{10}O_5 \cdot 5H_2O$ as reported by our group.[25] The vibration spectra of complexes **1** and **2** were assigned and interpreted in correlation with the crystal structures.

2. Experimental

2.1. Materials

$LaCl_3$ and $CeCl_3$ were prepared from corresponding rare earth oxide of high purity (99.99%).[32] D-Ribose was purchased from Acros, and was used without further purification.

2.2. Preparation of $LaCl_3 \cdot C_5H_{10}O_5 \cdot 5H_2O$ and $CeCl_3 \cdot C_5H_{10}O_5 \cdot 5H_2O$

D-Ribose (0.45 g, 3 mmol) and equivalent amounts of metal chlorides were dissolved in H_2O–EtOH, and the solutions were evaporated slowly until crystallization occurred. *Anal.* Calcd for $LaCl_3 \cdot C_5H_{10}O_5 \cdot 5H_2O$: C, 12.37; H, 4.15. Found: C, 12.14; H, 4.23. *Anal.* Calcd for $CeCl_3 \cdot C_5H_{10}O_5 \cdot 5H_2O$: C, 12.34; H, 4.14. Found: C, 12.22; H, 4.21.

2.3. Physical measurements

The mid-IR spectra were measured on a Nicolet Magna-IR 750 spectrometer using the micro-IR method, with 128 scans at 4 cm^{-1} resolution.

The structures of $LaCl_3$·ribopyranose·$5H_2O$ (**1**) and $CeCl_3$·ribopyranose·$5H_2O$ (**2**) were determined on a Bruker Smart 1000 diffractometer using monochromatic Mo Kα radiation ($\lambda = 0.71073$ Å) in the θ ranges from 2.07° to 26.42° (**1**) and from 2.07° to 26.41° (**2**) at 293 K, respectively. The final cycle of full-matrix least-squares refinements were based on 2649 observed reflections for (**1**) and 2906 observed reflections for (**2**). Calculations were completed with the SHELX-97 program.

Crystallographic data (without structure factors) for the structures reported in this paper have been deposited with the Cambridge Crystallographic Data Centre as supplementary publication no. CCDC-199655 (**1**) and no. CCDC-220665 (**2**). Copies of the data can be obtained free of charge on application to the CCDC, 12 Union Road, Cambridge CB2 1EZ, UK. [Fax: (internat.) +44-1223/336033; E-mail: deposit@ccdc.cam.ac.uk].

3. Results and discussion

3.1. X-Ray crystal structures

The crystal structures of the title complexes are isomorphous and are similar to that of $NdCl_3$·ribose·$5H_2O$.[25] The single crystals of the two complexes are both in disordered state in that two configurations, as a pair of anomers, were observed in each single crystal. The structures of complex **1** are shown in Figures 1 and 2; Figures 3 and 4 are of the two structures of **2**; Figures 5 and 6 are the projections of the crystal cells in the unit structures of **1** in which the ligand is the α-pyranose in $^4C_1$ configuration and **2** with which the ligand is the β-pyranose in $^1C_4$ configuration, respectively. The crystal data and structure refinements of the two complexes are listed in Table 1; selected bond lengths and angles of **1** are listed in Table 2, and those of **2** in Table 3.

Figures 1 and 3 show that the ribose moieties of complexes **1** and **2** are both α-pyranose in the $^4C_1$ conformation (abbreviated to αP^4C_1), which has been observed in $PrCl_3$·ribose·$5H_2O$[23] and $NdCl_3$·ribose·$5H_2O$.[24,25] Figures 2 and 4 show that the ribose moieties of the two complexes are both β-pyranose in $^1C_4$ conformation (abbreviated to βP^1C_4), which has only been observed in $NdCl_3 \cdot C_5H_{10}O_5 \cdot 5H_2O$.[25] For complex **1**, the α : β anomeric ratio is 51:49. For complex **2**, the anomeric ratio is 52:48. In both of the title complexes, the Ln ion (Ln = La or Ce) is nine coordinated and binds to three hydroxyl groups of one D-ribopyranose molecule, five water molecules, and a chloride ion. The other two Cl^- ions in the complex are free. The three adjacent hydroxyl groups, HO-1, 2, and 3 in the αP^4C_1 or HO-2, 3, and 4 in the βP^1C_4 both have the *ax–eq–ax* sequence as the coordination sites of D-ribose. The Ln–O dis-

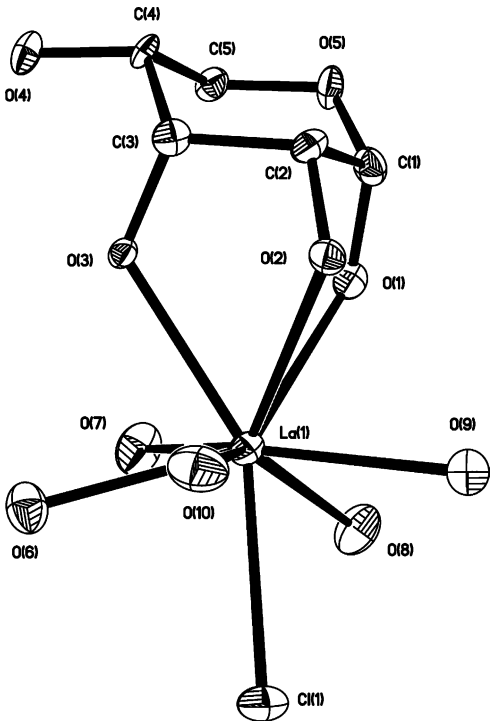

Figure 1. The structure and atom numbering scheme of $LaCl_3{\cdot}C_5H_{10}O_5{\cdot}5H_2O$ with which ligand in the αP^4C_1 configuration.

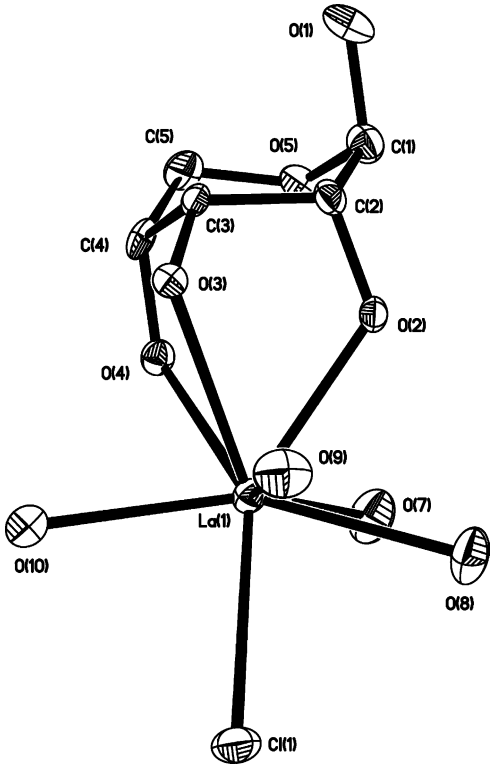

Figure 2. The structure and atom numbering scheme of $LaCl_3{\cdot}C_5H_{10}O_5{\cdot}5H_2O$ with which ligand in the βP^1C_4 configuration.

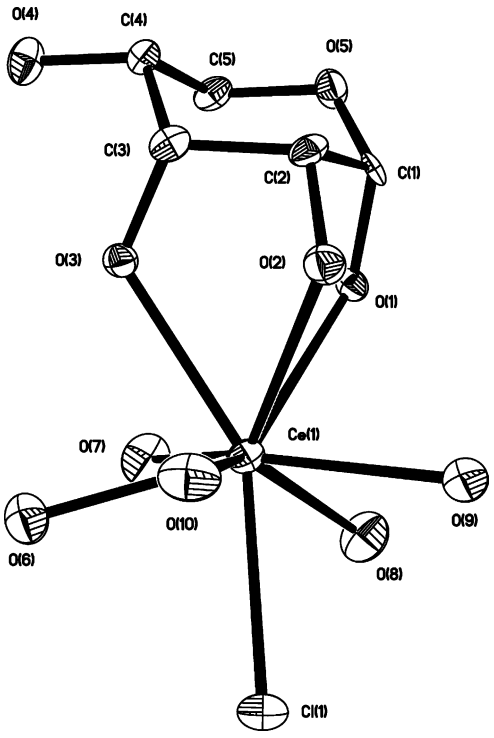

Figure 3. The structure and atom numbering scheme of $CeCl_3{\cdot}C_5H_{10}O_5{\cdot}5H_2O$ with which ligand in the αP^4C_1 configuration.

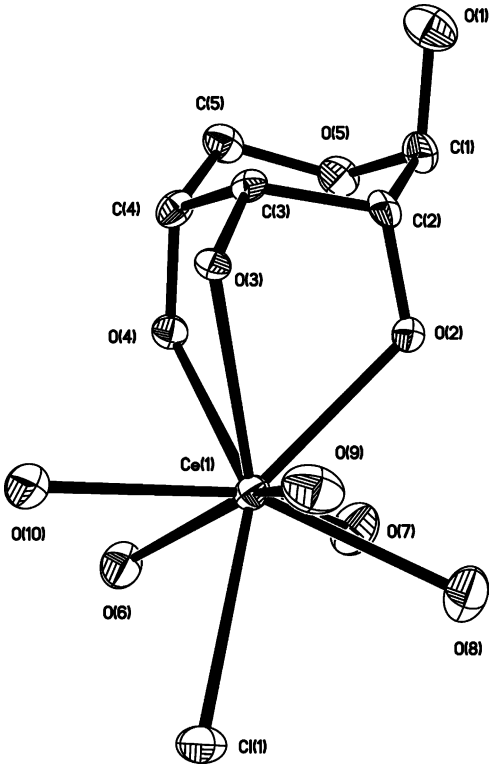

Figure 4. The structure and atom numbering scheme of $CeCl_3{\cdot}C_5H_{10}O_5{\cdot}5H_2O$ with which ligand in the βP^1C_4 configuration.

tances determined in this study (for **1**: from 2.513 to 2.690 Å; for **2**: from 2.484 to 2.690 Å) are comparable to those of Pr–O (from 2.480 to 2.594 Å)[23] and Nd–O (from 2.445 to 2.670 Å[25] or from 2.463 to 2.681 Å[24]). The

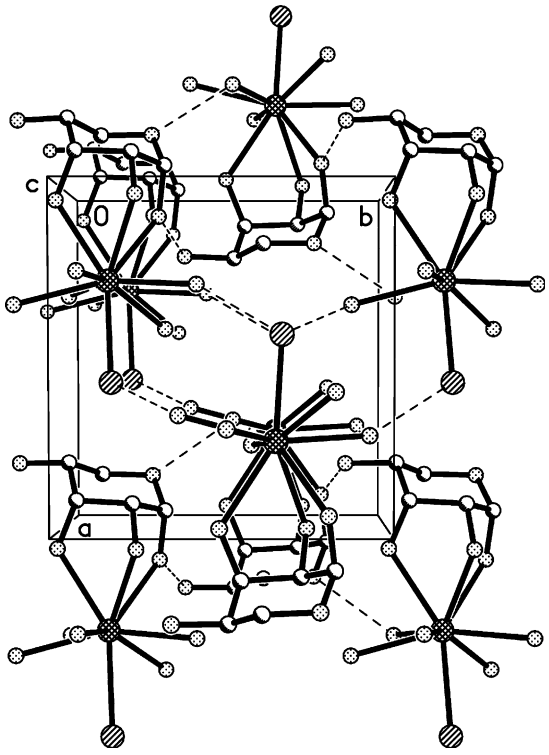

Figure 5. Projection of the crystal cell in the structure of $LaCl_3{\cdot}C_5H_{10}O_5{\cdot}5H_2O$ with which ligand in the αP^4C_1 configuration.

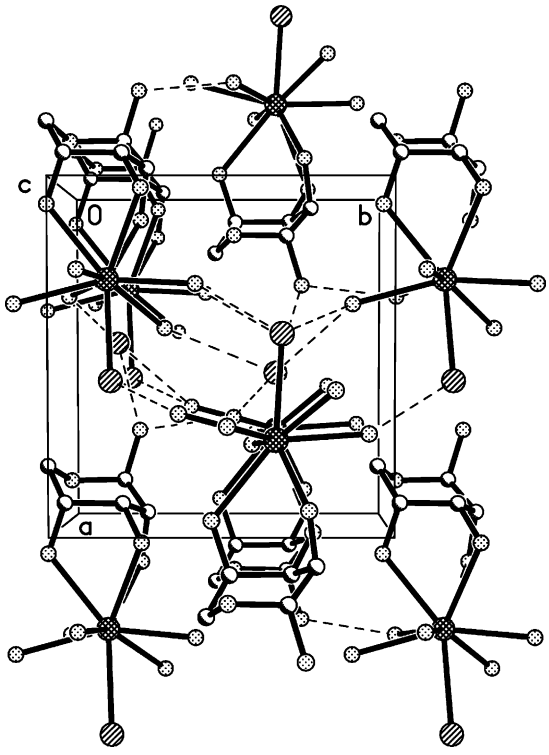

Figure 6. Projection of the crystal cell in the structure of $CeCl_3{\cdot}C_5H_{10}O_5{\cdot}5H_2O$ with which ligand in the βP^1C_4 configuration.

Table 1. Crystal data and structure refinement parameters for $LaCl_3{\cdot}C_5H_{10}O_5{\cdot}5H_2O$ and $CeCl_3{\cdot}C_5H_{10}O_5{\cdot}5H_2O$

Formula	$LaCl_3{\cdot}C_5H_{10}O_5{\cdot}5H_2O$	$CeCl_3{\cdot}C_5H_{10}O_5{\cdot}5H_2O$
Formula weight	485.47	486.68
Crystal system, Space group	Monoclinic, *P*2(1)	Monoclinic, *P*2(1)
a (Å)	9.281(3)	9.230(5)
b (Å)	8.847(3)	8.840(5)
c (Å)	9.849(3)	9.850(6)
β (°)	94.028(5)	93.996(9)
V (Å^3)	806.6(4)	801.6(8)
Z	2	2
D_{calcd} (Mg/m^3)	1.999	2.016
Absorption coefficient (mm^{-1})	3.181	3.375
F(000)	476	478
Crystal size (mm)	0.25×0.18×0.16	0.25×0.18×0.16
θ Range for data collection (°)	2.07–26.42	2.07–26.41
Index ranges	$-11 \leqslant h \leqslant 8$, $-9 \leqslant k \leqslant 11$, $-12 \leqslant l \leqslant 12$	$-8 \leqslant h \leqslant 11$, $-11 \leqslant k \leqslant 10$, $-12 \leqslant l \leqslant 6$
Reflections collected/unique	4636/2649 [*R*(int) = 0.0345]	4282/2906 [*R*(int) = 0.0362]
Completeness to θ	99.8% (θ = 26.42)	98.9% (θ = 26.41)
Absorption correction	Semi-empirical from equivalents	Semi-empirical from equivalents
Max/min transmission	0.6301 and 0.5035	0.6142 and 0.4858
Refinement method	Full-matrix least-squares on F^2	Full-matrix least-squares on F^2
S	1.013	0.958
Final *R* indices [$I > 2\sigma(I)$]	*R*1 = 0.0348, *wR*2 = 0.0612	*R*1 = 0.0347, *wR*2 = 0.0790
R indices (all data)	*R*1 = 0.0496, *wR*2 = 0.0652	*R*1 = 0.0429, *wR*2 = 0.0815
Absolute structure parameter	−0.02(2)	0.04(3)
Largest difference peak and hole (e/Å^3)	0.483 and −0.446	0.876 and −0.681
Data/restraints/parameters	2649/585/265	2906/579/265
α,β anomer ratio	51/49	52/48

torsion angles of the ribose moiety in **1**, **2**, and $NdCl_3{\cdot}C_5H_{10}O_5{\cdot}5H_2O$[25] are similar (see Table 4), indicating that the sugar ring is not much changed by the metal-ion coordination. As no data have been reported

Table 2. Selected bond lengths (Å) and angles (°) for $LaCl_3{\cdot}C_5H_{10}O_5{\cdot}5H_2O$[a]

La(1)–O(2′)	2.513(13)	O(5)–C(5)	1.444(12)
La(1)–O(9)	2.518(5)	O(5)–C(1)	1.442(12)
La(1)–O(6)	2.531(5)	C(1)–C(2)	1.536(9)
La(1)–O(10)	2.539(5)	C(2)–C(3)	1.531(8)
La(1)–O(7)	2.542(5)	C(3)–C(4)	1.524(8)
La(1)–O(4′)	2.559(17)	C(4)–C(5)	1.535(9)
La(1)–O(2)	2.56(2)	O(1′)–C(1′)	1.420(13)
La(1)–O(8)	2.572(5)	O(2′)–(2′)	1.417(11)
La(1)–O(3)	2.593(15)	O(3′)–C(3′)	1.440(12)
La(1)–O(1)	2.643(13)	O(4′)-C(4′)	1.430(12)
La(1)–O(3′)	2.69(2)	O(5′)–C(1′)	1.442(12)
La(1)–Cl(1)	2.834(18)	O(5′)–C(5′)	1.439(13)
O(1)–C(1)	1.418(11)	C(1′)–C(2′)	1.530(9)
O(2)–C(2)	1.428(12)	C(2′)–C(3′)	1.528(9)
O(3)–C(3)	1.437(12)	C(3′)–C(4′)	1.525(8)
O(4)–C(4)	1.421(11)	C(4′)–C(5′)	1.526(9)
O(2′)–La(1)–O(9)	87.2(3)	O(7)–La(1)–Cl(1)	100.76(15)
O(2′)–La(1)–O(6)	123.4(3)	O(4′)–La(1)–Cl(1)	141.8(4)
O(9)–La(1)–O(6)	149.06(16)	O(2)–La(1)–Cl(1)	132.0(4)
O(2′)–La(1)–O(10)	132.1(3)	O(8)–La(1)–Cl(1)	74.77(14)
O(9)–La(1)–O(10)	84.64(18)	O(3)–La(1)–Cl(1)	149.5(3)
O(6)–La(1)–O(10)	71.34(16)	O(1)–La(1)–Cl(1)	142.2(3)
O(2′)–La(1)–O(7)	70.8(3)	O(3′)–La(1)–Cl(1)	134.0(4)
O(9)–La(1)–O(7)	136.80(18)	C(1)–O(1)–La(1)	122.7(10)
O(6)–La(1)–O(7)	66.72(17)	C(2)–O(2)–La(1)	116.4(16)
O(10)–La(1)–O(7)	137.57(18)	C(3)–O(3)–La(1)	121.3(11)
O(2′)–La(1)–O(4′)	69.2(4)	C(1)–O(5)–C(5)	116.4(11)
O(9)–La(1)–O(4′)	128.7(4)	O(1)–C(1)–O(5)	111.5(12)
O(6)–La(1)–O(4′)	67.0(4)	O(1)–C(1)–C(2)	109.0(13)
O(10)–La(1)–O(4′)	79.9(3)	O(5)–C(1)–C(2)	111.5(10)
O(7)–La(1)–O(4′)	78.2(4)	O(2)–C(2)–C(3)	104.5(17)
O(9)–La(1)–O(2)	67.8(4)	O(2)–C(2)–C(1)	107.1(16)
O(6)–La(1)–O(2)	118.0(5)	C(3)–C(2)–C(1)	111.2(8)
O(10)–La(1)–O(2)	68.7(5)	O(3)–C(3)–C(4)	110.2(13)
O(7)–La(1)–O(2)	127.3(4)	O(3)–C(3)–C(2)	111.1(14)
O(2′)–La(1)–O(8)	72.8(3)	C(4)–C(3)–C(2)	111.3(7)
O(9)–La(1)–O(8)	71.19(18)	O(4)–C(4)–C(3)	112.0(12)
O(6)–La(1)–O(8)	119.23(16)	O(4)–C(4)–C(5)	107.0(10)
O(10)–La(1)–O(8)	145.08(18)	C(3)–C(4)–C(5)	111.1(8)
O(7)–La(1)–O(8)	66.99(16)	O(5)–C(5)–C(4)	108.8(10)
O(4′)–La(1)–O(8)	135.0(3)	C(2′)–O(2′)–La(1)	123.9(10)
O(2)–La(1)–O(8)	120.8(5)	C(3′)–O(3′)–La(1)	106.5(15)
O(9)–La(1)–O(3)	126.8(3)	C(4′)–O(4′)–La(1)	123.7(12)
O(6)–La(1)–O(3)	72.9(3)	C(5′)–O(5′)–C(1′)	116.3(12)
O(10)–La(1)–O(3)	88.1(3)	O(1′)–C(1′)–O(5′)	107.8(11)
O(7)–La(1)–O(3)	74.0(3)	O(1′)–C(1′)–C(2′)	107.3(12)
O(2)–La(1)–O(3)	60.6(6)	O(5′)–C(1′)–C(2′)	113.0(9)
O(8)–La(1)–O(3)	126.5(3)	O(2′)–C(2′)–C(3′)	109.1(13)
O(9)–La(1)–O(1)	76.6(3)	O(2′)–C(2′)–C(1′)	106.7(12)
O(6)–La(1)–O(1)	133.8(3)	C(3′)–C(2′)–C(1′)	111.6(8)
O(10)–La(1)–O(1)	128.3(3)	O(3′)–C(3′)–C(4′)	113.6(16)
O(7)–La(1)–O(1)	80.1(3)	O(3′)–C(3′)–C(2′)	104.1(15)
O(2)–La(1)–O(1)	59.5(5)	C(4′)–C(3′)–C(2′)	112.5(8)
O(8)–La(1)–O(1)	70.9(3)	O(4′)–C(4′)–C(3′)	108.0(14)
O(3)–La(1)–O(1)	67.5(4)	O(4′)–C(4′)–C(5′)	115.2(16)
O(2′)–La(1)–O(3′)	60.2(5)	C(3′)–C(4′)–C(5′)	111.8(8)
O(9)–La(1)–O(3′)	66.0(4)	O(5′)–C(5′)–C(4′)	106.6(11)
O(6)–La(1)–O(3′)	122.1(5)	O(2′)–La(1)–Cl(1)	147.2(3)
O(10)–La(1)–O(3′)	73.5(5)	O(9)–La(1)–Cl(1)	77.87(15)
O(7)–La(1)–O(3′)	125.0(4)	O(6)–La(1)–Cl(1)	77.52(16)
O(4′)–La(1)–O(3′)	62.6(6)	O(10)–La(1)–Cl(1)	75.77(12)
O(8)–La(1)–O(3′)	116.1(5)		

[a] To distinguish atoms of the ribose moieties between the two isomers, the atoms in the $\beta P^1 C_4$ configuration are numbered with a prime, and so are the atoms in the below tables.

Table 3. Selected bond lengths (Å) and angles (°) for $CeCl_3{\cdot}C_5H_{10}O_5{\cdot}5H_2O$

Ce(1)–O(2′)	2.484(13)	O(5)–C(5)	1.442(12)
Ce(1)–O(9)	2.488(6)	O(5)–C(1)	1.437(11)
Ce(1)–O(6)	2.511(6)	C(1)–C(2)	1.529(9)
Ce(1)–O(10)	2.516(6)	C(2)–C(3)	1.527(8)
Ce(1)–O(2)	2.530(3)	C(3)–C(4)	1.536(8)
Ce(1)–O(7)	2.528(6)	C(4)–C(5)	1.537(9)
Ce(1)–O(4′)	2.543(17)	O(1′)–C(1′)	1.421(14)
Ce(1)–O(8)	2.557(6)	O(2′)–C(2′)	1.418(12)
Ce(1)–O(3)	2.583(14)	O(3′)–C(3′)	1.433(12)
Ce(1)–O(1)	2.624(11)	O(4′)–C(4′)	1.424(12)
Ce(1)–O(3′)	2.690(3)	O(5′)–C(1′)	1.444(13)
Ce(1)–Cl(1)	2.813(2)	O(5′)–C(5′)	1.437(13)
O(1)–C(1)	1.414(11)	C(1′)–C(2′)	1.532(9)
O(2)–C(2)	1.429(12)	C(2′)–C(3′)	1.524(9)
O(3)–C(3)	1.441(12)	C(3′)–C(4′)	1.527(9)
O(4)–C(4)	1.420(12)	C(4′)–C(5′)	1.531(9)
O(2′)–Ce(1)–O(9)	88.0(3)	O(8)–Ce(1)–O(3)	127.0(3)
O(2′)–Ce(1)–O(6)	123.1(3)	O(9)–Ce(1)–O(1)	77.1(3)
O(9)–Ce(1)–O(6)	148.62(18)	O(6)–Ce(1)–O(1)	133.7(3)
O(2′)–Ce(1)–O(10)	133.3(3)	O(10)–Ce(1)–O(1)	127.6(3)
O(9)–Ce(1)–O(10)	84.3(2)	O(2)–Ce(1)–O(1)	58.0(7)
O(6)–Ce(1)–O(10)	71.68(19)	O(7)–Ce(1)–O(1)	80.6(3)
O(9)–Ce(1)–O(2)	67.3(6)	O(8)–Ce(1)–O(1)	71.8(3)
O(6)–Ce(1)–O(2)	119.6(8)	O(3)–Ce(1)–O(1)	67.0(4)
O(10)–Ce(1)–O(2)	69.6(7)	O(2′)–Ce(1)–O(3′)	63.0(6)
O(2′)–Ce(1)–O(7)	70.0(3)	O(9)–Ce(1)–O(3′)	66.7(6)
O(9)–Ce(1)–O(7)	136.3(2)	O(6)–Ce(1)–O(3′)	121.3(7)
O(6)–Ce(1)–O(7)	66.8(2)	O(10)–Ce(1)–O(3′)	71.7(6)
O(10)–Ce(1)–O(7)	138.1(2)	O(7)–Ce(1)–O(3′)	126.6(5)
O(2)–Ce(1)–O(7)	127.7(5)	O(4′)–Ce(1)–O(3′)	63.1(7)
O(2′)–Ce(1)–O(4′)	70.2(5)	O(8)–Ce(1)–O(3′)	117.6(7)
O(9)–Ce(1)–O(4′)	129.8(4)	O(2′)–Ce(1)–Cl(1)	146.5(3)
O(6)–Ce(1)–O(4′)	66.5(4)	O(9)–Ce(1)–Cl(1)	77.39(15)
O(10)–Ce(1)–O(4′)	80.0(4)	O(6)–Ce(1)–Cl(1)	77.26(17)
O(7)–Ce(1)–O(4′)	78.5(4)	O(10)–Ce(1)–Cl(1)	75.61(12)
O(2′)–Ce(1)–O(8)	72.0(3)	O(2)–Ce(1)–Cl(1)	132.0(5)
O(9)–Ce(1)–O(8)	71.0(2)	O(7)–Ce(1)–Cl(1)	100.31(16)
O(6)–Ce(1)–O(8)	118.94(19)	O(4′)–Ce(1)–Cl(1)	141.1(4)
O(10)–Ce(1)–O(8)	144.8(2)	O(8)–Ce(1)–Cl(1)	74.77(15)
O(2)–Ce(1)–O(8)	119.6(8)	O(3)–Ce(1)–Cl(1)	149.6(3)
O(7)–Ce(1)–O(8)	66.5(2)	O(1)–Ce(1)–Cl(1)	142.9(3)
O(4′)–Ce(1)–O(8)	135.2(4)	O(3′)–Ce(1)–Cl(1)	133.0(4)
C(3′)–O(3′)–Ce(1)	104.2(18)	C(1)–O(1)–Ce(1)	125.9(9)
O(9)–Ce(1)–O(3)	126.9(3)	C(2)–O(2)–Ce(1)	118(2)
O(6)–Ce(1)–O(3)	73.3(3)	C(3)–O(3)–Ce(1)	120.4(10)
O(10)–Ce(1)–O(3)	87.8(3)	C(1)–O(5)–C(5)	116.6(10)
O(2)–Ce(1)–O(3)	60.8(7)	O(1)–C(1)–O(5)	112.3(11)
O(7)–Ce(1)–O(3)	75.1(3)	O(1)–C(1)–C(2)	105.9(12)
C(4′)–O(4′)–Ce(1)	122.6(12)	O(5)–C(1)–C(2)	110.2(9)
C(2′)–O(2′)–Ce(1)	120.9(10)	O(2)–C(2)–C(3)	103.2(18)
O(3′)–C(3′)–C(4′)	112.8(18)	O(2)–C(2)–C(1)	106.5(19)
C(2′)–C(3′)–C(4′)	112.6(8)	C(3)–C(2)–C(1)	112.1(8)
O(4′)–C(4′)–C(3′)	107.8(13)	O(3)–C(3)–C(2)	112.2(14)
C(5′)–O(5′)–C(1′)	116.5(12)	O(3)–C(3)–C(4)	109.0(12)
O(4′)–C(4′)–C(5′)	113.9(15)	C(2)–C(3)–C(4)	111.0(7)
C(3′)–C(4′)–C(5′)	111.4(8)	O(4)–C(4)–C(3)	112.6(11)
O(5′)–C(5′)–C(4′)	107.5(11)	O(4)–C(4)–C(5)	105.4(10)
O(5)–C(5)–C(4)	106.4(10)	C(3)–C(4)–C(5)	110.0(7)
C(3′)–C(2′)–C(1′)	111.5(8)	O(2′)–C(2′)–C(1′)	106.8(12)
O(1′)–C(1′)–O(5′)	107.4(12)	O(2′)–C(2′)–C(3′)	111.3(13)
O(3′)–C(3′)–C(2′)	106.3(19)	O(1′)–C(1′)–C(2′)	111.2(12)
O(5′)–C(1′)–C(2′)	112.0(10)		

Table 4. Selected torsion angles (°) for $LaCl_3{\cdot}C_5H_{10}O_5{\cdot}5H_2O$, $CeCl_3{\cdot}C^5H_{10}O_5{\cdot}5H_2O$, and $NdCl_3{\cdot}C_5H_{10}O_5{\cdot}5H_2O$[a]

Configuration and conformation of the ribopyranose moiety	Torsion angles	Ribose–La	Ribose–Ce	Ribose–Nd[a]
$\alpha P^4\, C_1$	C(5)–O(5)–C(1)–C(2)	−55.5(17)	−58.2(16)	−57.6(13)
	O(5)–C(1)–C(2)–C(3)	49.5(17)	48.5(16)	52.7(14)
	C(1)–C(2)–C(3)–C(4)	−50.3(17)	−49.4(17)	−53.1(15)
	C(2)–C(3)–C(4)–C(5)	54.1(15)	55.3(14)	54.9(13)
	C(1)–O(5)–C(5)–C(4)	58.0(17)	63.2(16)	60.4(14)
	C(3)–C(4)–C(5)–O(5)	−55.8(16)	−59.2(15)	−57.3(13)
$\beta P^1\, C_4$	C(5)–O(5)–C(1)–C(2)	55.6(18)	56.2(18)	58.6(13)
	O(5)–C(1)–C(2)–C(3)	−44.2(17)	−46.4(17)	−45.3(13)
	C(1)–C(2)–C(3)–C(4)	44.4(17)	46.4(17)	44.1(13)
	C(2)–C(3)–C(4)–C(5)	−53.0(17)	−52.6(17)	−52.2(15)
	C(1)–O(5)–C(5)–C(4)	−61.1(18)	−60.4(18)	−62.8(13)
	C(3)–C(4)–C(5)–O(5)	58.4(17)	56.8(17)	57.3(14)

[a] From our unpublished data.

on the crystal structure of D-ribose in the literature, and so we cannot calculate changes in the torsion angles of the sugar ring upon metalation. The ring oxygen atoms of D-ribose does not coordinate with Ln^{3+} in either of the complexes. All water molecules are coordinated in the two complexes. The coordination behavior of La^{3+}, Ce^{3+}, Pr^{3+}, and Nd^{3+} are shown to be similar from the X-ray results.

As expected, there is an extensive network of hydrogen bonds involving all hydroxyl groups, water molecules, and chloride ions in the crystals of **1** and **2** (see Tables 5 and 6). The Ln–ribose complexes are organized by these hydrogen bonds and thus form layers parallel to the (1 0 −1) plane. These layers are then also held together by hydrogen bonds with regular spaces between them. Free Cl ions distributed in these layers are responsible for not only the formation of a layer but also the bonding between the layers by hydrogen bonds. This network of hydrogen bonds forms the packed structure of the whole crystal. In the title complexes, the Cl^- ions play important roles not only as counterions but also as the predominant feature in the network of hydrogen bonds.

Table 5. Hydrogen bonds for $LaCl_3{\cdot}C_5H_{10}O_5{\cdot}5H_2O$ with $H\cdots A < r(A) + 2.000$ Å and $<DHA > 110°$

D–H···A	d(D–H)	d(H···A)	d(D···A)	<(DHA)
O6–H6A···Cl3#1	0.851	2.505	3.170	135.56
O6–H6B···Cl2#2	0.850	2.720	3.522	157.85
O7–H7B···O5#3	0.846	2.059	2.883	164.42
O7–H7B···O1′#3	0.846	2.104	2.723	129.56
O8–H8A···Cl3	0.842	2.388	3.224	172.09
O8–H8B···O4#4	0.842	2.282	2.998	143.09
O8–H8B···Cl3#2	0.842	2.742	3.409	137.33
O9–H9A···Cl1#5	0.848	2.422	3.172	147.76
O9–H9B···Cl2#6	0.848	2.325	3.170	173.46
O10–H10A···Cl3#7	0.852	2.632	3.245	129.95
O10–H10A···Cl1	0.852	2.916	3.308	110.18
O10–H10B···Cl2#8	0.853	2.296	3.101	157.32
O1–H1···O4#4	0.930	1.736	2.646	165.14
O2–H2···Cl2#8	0.930	2.328	2.979	126.74
O3–H3···Cl2#2	0.930	2.516	3.162	126.85
O4–H4···Cl3#9	0.820	2.413	3.219	167.66
O1′–H1′···O7#4	0.820	1.945	2.723	158.14
O2′–H2′···O5′#4	0.930	2.365	2.934	119.23
O3′–H3′···Cl2#8	0.930	2.729	3.127	106.80
O4′–H4′···Cl2#2	0.930	2.088	2.914	147.28

Symmetry transformations used to generate equivalent atoms: #1 $x, y-1, z$#2; $-x+1, y-1/2, -z+1$; #3 $-x, y-1/2, -z+1$; #4 $-x, y+1/2, -z+1$; #5 $-x+1, y+1/2, -z+2$; #6 $-x+1, y+1/2, -z+1$; #7 $-x+1, y-1/2, -z+2$; #8 $x-1, y, z+1$; #9 $x-1, y-1, z$.

Table 6. Hydrogen bonds for $CeCl_3{\cdot}C_5H_{10}O_5{\cdot}5H_2O$ with $H\cdots A < r(A) + 2.000$ Å and $<DHA > 110°$

D–H···A	d(D–H)	d(H···A)	d(D···A)	<(DHA)
O6–H6A···Cl3#1	0.847	2.514	3.173	135.35
O6–H6B···Cl2#2	0.848	2.718	3.519	158.25
O7–H7B···O5#3	0.844	2.092	2.913	164.06
O7–H7B···O1′#3	0.844	2.114	2.737	130.31
O8–H8A···Cl3	0.841	2.381	3.216	172.19
O8–H8B···O4#4	0.841	2.300	3.015	142.96
O8–H8B···Cl3#2	0.841	2.759	3.430	137.93
O9–H9A···Cl1#5	0.846	2.437	3.184	147.68
O9–H9B···Cl2#6	0.845	2.338	3.179	173.06
O10–H10A···Cl3#7	0.850	2.643	3.250	129.47
O10–H10A···Cl1	0.850	2.885	3.275	110.01
O10–H10B···Cl2#8	0.850	2.285	3.089	157.87
O1–H1···O4#4	0.930	1.771	2.689	168.97
O2–H2···Cl2#8	0.930	2.412	3.036	124.38
O3–H3···Cl2#2	0.930	2.509	3.169	128.18
O4–H4···Cl3#9	0.820	2.541	3.221	141.20
O1′–H1′···O8#10	0.820	2.768	3.160	159.10
O2′–H2′···O5′#4	0.930	2.390	2.936	117.41
O3′–H3′···Cl2#8	0.930	2.617	3.059	109.70
O4′–H4′···Cl2#2	0.930	2.087	2.900	145.38

Symmetry transformations used to generate equivalent atoms: #1 $x, y-1, z$; #2 $-x+1, y-1/2, -z+1$; #3 $-x, y-1/2, -z+1$; #4 $-x, y+1/2, -z+1$; #5 $-x+1, y+1/2, -z+2$; #6 $-x+1, y+1/2, -z+1$; #7 $-x+1, y-1/2, -z+2$; #8 $x-1, y, z+1$; #9 $x-1, y-1, z$; #10 $x-1, y, z$.

3.2. IR spectroscopy studies of La–ribose and Ce–ribose complexes

The FT-IR spectra of D-ribose and the La^{3+}, Ce^{3+}, and Nd^{3+} complexes are shown in Figure 7. The absorption bands and tentative assignments are given in Table 7.

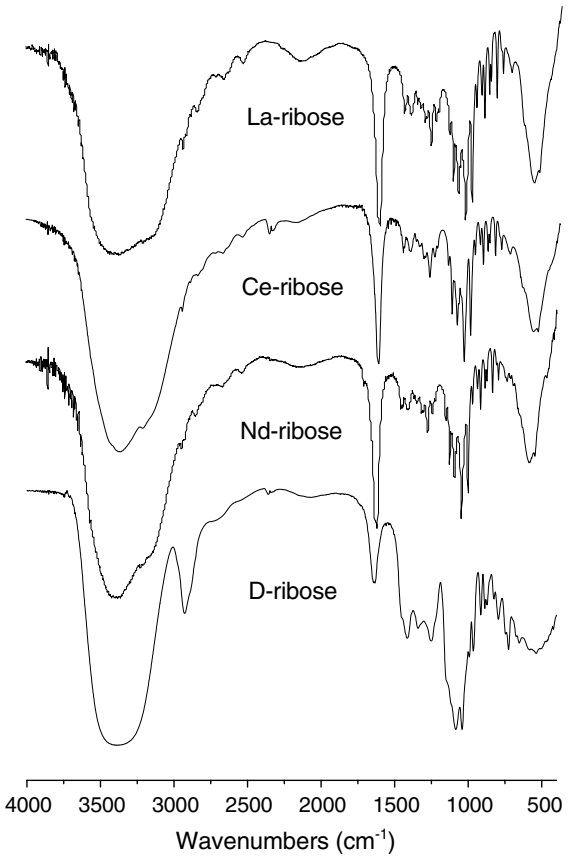

Figure 7. The mid-IR spectra of D-ribose, La–, Ce–, and Nd–D-ribose.

The IR data of La–, Ce–, and Nd–ribose are similar, indicating that La^{3+}, Ce^{3+}, and Nd^{3+} have similar coordination modes. The broad absorption band around 3400 cm^{-1} in the spectrum of D-ribose can be assigned to the hydrogen-bonded OH groups. This band appears broader in the spectra of the metal complexes (see Fig. 7). The observed spectral changes are due to the metalation of the sugar and the rearrangement of the strong hydrogen-bonding network in the crystal structures of the complexes (see Tables 5 and 6). The C–H stretching vibration bands (for La–ribose: 2946, 2853, 2673, 2539 cm^{-1}, for Ce–ribose: 2946, 2853, 2672, 2541 cm^{-1}) in the spectra of the complexes, corresponding to the band of 2928 cm^{-1} in the spectrum of free D-ribose, are observed weaker and are masked by the broadened *v*OH bands. The bands at about 1622 cm^{-1} in the spectra of the complexes can be assigned to the δ_{HOH} vibration of the coordinated water. The bands at 1452, 1417, 1340, 1250 cm^{-1} in the spectrum of free D-ribose, assigned to the multiple bending vibrations of O–C–H, C–C–H, C–O–H, and CH_2, are shifted in the spectra of the complexes, and their intensities become weaker upon salt formation (see Table 7). The band at about 1150 cm^{-1} is the characteristic vibration of a pyranose,[33] and is observed in the spectra of the complexes and D-ribose itself. In the 1200–970 cm^{-1} region, the C–O, C–C stretching vibrations, and the C–O–H, C–C–O bending vibrations, of D-ribose are observed to be shifted and split in the spectra of the complexes (see Table 7). Such observed splitting and shifting is indicative of the participation of the sugar hydroxyl groups in metal–ligand bonding, which therefore affects the C–O, C–C stretching vibrations and the C–O–H, C–C–O bending vibrations of the sugar moiety.

The ring skeletal deformation bands (δC–C–O and δC–C-C) of free D-ribose, mainly in the 1000–400 cm^{-1} region, show considerable changes on complex formation (see Fig. 7 and Table 7). This may be attributed to distortion of the sugar ring upon metalation. However, no crystal data for free D-ribose have been reported to permit comparison with those of the complexes. The spectral changes observed in this region may be

Table 7. IR data for D-ribose, La–ribose, Ce–ribose, Pr–ribose, and Nd–ribose complexes (1500–700 cm^{-1})

D-Ribose	La–ribose	Ce–ribose	Pr–ribose[23]	Nd–ribose[25]	Possible assignment[33–38]
1452	1457	1458	1458	1456	δOCH + δCCH + δCH_2
1417	1410	1417	1409	1408	δOCH + δCCH
1340	1348	1348	1350	1350	δOCH + δCCH + δCOH
	1319	1318	1318	1315	δOCH + δCCH + δCOH
1250	1244	1244	1244	1244	δCCH + δCOH + δOCH
1153	1152	1153	1152	1153	νC–O + νC–C + δCOH (pyranose)
1117	1128	1127	1128	1128	νC–O + νC–C + δCOH
1085	1093	1094	1095	1091	νC–O + νC–C + δCOH
1042	1047	1047	1048	1047	νC–O + νC–C + δCCO
	1004	1004	1004	1003	ν C–O + νC–C + δCCO
987	971	971	972	971	νC–O + νC–C + δCCO
914	917	917	918	918	νC–O + δCCH + ν asy(ring of pyranose)
887	885	886	887	888	νC–O + νC–C + δCCH
872	874	874	874	874	δCH(β-pyranose)
	835	835	836	836	δCH(α-pyranose)
826					δCH
795	793	794	795	796	τC–O + δCCO + δCCH + ν sy(ring of pyranose)
746	734	735	736	734	τC–O + δCCO + δCCH

δ, bending mode; ν, stretching mode; τ, twisting.

interpreted to indicate that metalation of the sugar perturbs the electron distribution within the sugar ring system, where the vibrations are mostly localized, and finally causes ring distortion, resulting in the alterations in the spectra. The 914 and 795 cm^{-1} bands in the D-ribose spectrum are attributed to the asymmetric and symmetric ring-breathing modes of the pyranose, respectively. They are observed as bands at around 917 and 794 cm^{-1} in the spectrum of each complex (see Table 7), indicating that the six-membered sugar ring is retained in each complex. The absorption bands at about 870 and 840 cm^{-1} in a pyranose spectrum are generally assigned to the presence of the β and α anomers, respectively.[34,35] In relation to the spectra of the Ln–D-ribose complex, the coexistence of the absorption bands at about 874 and 835 cm^{-1} in each spectrum indicates that the complex is, in fact, a mixture with both α-ribopyranose and β-ribopyranose as ligands. The two configurations of the complex indicated by the IR data are in accord with the X-ray results.

The IR results indicate that the hydroxyl groups of D-ribose take part in the metal–oxygen interaction; the hydrogen-bond network rearranges upon metalation; and there are two isomers coexisting in the complex with both α-ribopyranose and β-ribopyranose as ligands. The IR results are in accord with those of X-ray diffraction, and the FT-IR technique is thus a useful method for detecting the formation of such complexes.

References

1. Luo, J. S. *Biochemistry*; Huadong Normal University Press: Shanghai, 1997.
2. Templeton, D. M.; Sarkar, B. *Biochem. J.* **1985**, *230*, 35–42.
3. Sauchelli, V. *Trace Elements in Agriculture*; Van Nostrand: New York, 1969. p 248.
4. Holm, R. P.; Berg, J. M. *Pure Appl. Chem.* **1984**, *56*, 1645–1657.
5. Predki, P. F.; Whitfield, D. M.; Sarkar, B. *Biochem. J.* **1992**, *281*, 835–841.
6. Templeton, D. M.; Sarkar, B. *Biochem. J.* **1985**, *230*, 35–42.
7. Weis, W. I.; Drickamer, K.; Hendrickson, W. A. *Nature* **1992**, *360*, 127–134.
8. Drickamer, K. *Nature* **1992**, *360*, 183–186.
9. Taylor, G. E.; Waters, J. M. *Tetrahedron Lett.* **1981**, *22*, 1277–1278.
10. Craig, D. C.; Stephenson, N. C.; Stevens, J. D. *Cryst. Struct. Commun.* **1974**, *3*, 277–281.
11. Craig, D. C.; Stephenson, N. C.; Stevens, J. D. *Cryst. Struct. Commun.* **1974**, *3*, 195–199.
12. Cook, W. J.; Bugg, C. E. *Acta Cryst.* **1976**, *32*, 656–659.
13. Cook, W. J.; Bugg, C. E. *J. Am. Chem. Soc.* **1973**, *95*, 6442–6446.
14. Bugg, C. E. *J. Am. Chem. Soc.* **1973**, *95*, 908–913.
15. Cook, W. J.; Bugg, C. E. *Acta Crystallogr., Sect. B.* **1973**, *29*, 907–909.
16. Accorsi, C. A.; Bertolasi, V.; Ferretti, V.; Gastone, G. *Carbohydr. Res.* **1989**, *191*, 91–104.
17. Accorsi, C. A.; Bellucci, F.; Bertolasi, V.; Valeria, F.; Gastone, G. *Carbohydr. Res.* **1989**, *191*, 105–116.
18. Peralta-Inga, Z.; Johnson, G. P.; Dowd, M. K., Rendleman, J. A.; Stevens, E. D.; French, A. D. *Carbohydr. Res.* **2002**, *337*, 851–861.
19. Craig, D. C.; Stephenson, N. C.; Stevens, J. D. *Carbohydr. Res.* **1972**, *22*, 494–495.
20. Cook, W. J.; Bugg, C. E. *Carbohydr. Res.* **1973**, *31*, 265–275.
21. Richards, G. F. *Carbohydr. Res.* **1973**, *26*, 448–449.
22. Terzis, A. *Cryst. Struct. Commun.* **1978**, *7*, 95–99.
23. Yang, L. M.; Zhao, Y.; Xu, Y. Z.; Jin, X. L.; Weng, S. F.; Wen, T.; Wu, J. G.; Xu, G. X. *Carbohydr. Res.* **2001**, *334*, 91–95.
24. Yang, L. M.; Wu, J. G.; Weng, S. F.; Jin, X. L. *J. Mol. Struct.* **2002**, *612*, 49–57.
25. Lu, Y.; Deng, G. C.; Miao, F. M.; Li, Z. M. *Carbohydr. Res.* **2003**, *338*, 2913–2919.
26. Lu, Y.; Deng, G. C.; Miao, F. M.; Li, Z. M. *J. Inorg. Biochem.* **2003**, *96*, 487–492.
27. Angyal, S. J. *Pure Appl. Chem.* **1973**, *35*, 131–146.
28. Alvarez, A. M.; Desrosiers, N. M.; Morel, J. P. *Can. J. Chem.* **1987**, *65*, 2656–2660.
29. Desrosiers, N. M.; Lhermet, C.; Morel, J. P. *J. Chem. Soc., Faraday Trans.* **1991**, *87*, 2173–2177.
30. Desrosiers, N. M.; Lhermet, C.; Morel, J. P. *J. Chem. Soc., Faraday Trans.* **1993**, *89*, 1223–1228.
31. Su, Y. L.; Yang, L. M.; Weng, S. F.; Wu, J. G. *J. Rare Earths.* **2002**, *20*, 339–342.
32. Chandrasekhar, A. *J. Imaging Technol.* **1990**, *16*, 158–161.
33. Cael, J. J.; Koenig, J. L.; Blackwell, J. *Carbohydr. Res.* **1974**, *32*, 79–91.
34. Tajmir-Riahi, A. H. *Carbohydr. Res.* **1983**, *122*, 241–248.
35. Tajmir-Riahi, A. H. *Carbohydr. Res.* **1984**, *127*, 1–8.
36. Zhang, W. J. *Biochemical Technology of Complexes of Carbohydrate*; Zhejiang University Press: Hangzhou, 1999. pp 193–198.
37. Mathlouthi, M.; Seuvre, A. M.; Koenig, J. L. *Carbohydr. Res.* **1983**, *122*, 31–47.
38. Tajmir-Riahi, A. H. *Biophys. Chem.* **1986**, *23*, 223–228.